# Chapter 2
Grind-Hardening State-of-the-Art

Abstract Grind-hardening process has a history of almost 20 years. Since its introduction, numerous studies have been presented focusing on a number of aspects of the process such as the modelling of the process, the impact of the process parameters, the grinding wheel importance, etc. In the present chapter, the relevant literature to grind-hardening process is classified and summarized. More than 100 papers have been reviewed.

2.1 Introduction

In conventional grinding of hardened steels, the thermal impact on the surface layer can result in surface layer damages due to structural alterations by annealing or re-hardening. By annealing, the surface layer hardness can be reduced significantly, which causes a decrease of the wear resistance and rolling contact strength. Due to the extreme hard and brittle martensitic structure at the surface and an annealed zone lying beneath, re-hardened layers are characterized by very steep hardness gradients. Combined with surface stresses, this can cause crack initiation and crack propagation. In contrast to this, in grind hardening the heat dissipated in the contact zone between grinding wheel and workpiece is used for the material's surface layer austenitization. The critical cooling rate demanded for martensitic hardening of the austenitized surface layer is mainly achieved by self-quenching mechanism and supported by the ambient cooling lubricant. Due to the kinematical contact conditions in grinding, grind hardening is a short-time metallurgical process applying austenitization durations of splits of seconds.

Grind-hardening process is a relatively new one that was introduced by Brinksmeier and Brockhoff [1] in mid 1990s. However, the possibility of using the heat generated during grinding for changing the material's structure had been already studied by Eda et al. [2], Shaw and Vyas [3], and Zhang and Mahdi [4]. Since the introduction of the process, the interest in the process has been increased internationally as can be seen in Fig. 2.1 by the rising numbers of publications. Since 1995, 112 relevant publications were collected through searching scientific paper databases

Fig. 2.1 Results of the
literature research
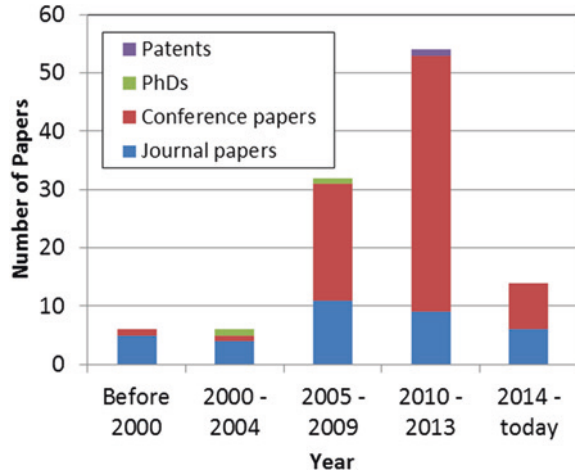
(such as Scopus, Web of Science, Google Scholar etc.) and scientific publishers'
archives. 30 % of these papers have been published in scientific journals whereas the
rest were presented in scientific conferences after review. Two PhD theses and a pat-
ent on the grind-hardening process were also found. The present chapter highlights
the state of the art with regards the grind-hardening process since its introduction in
1995. In a recent study, Klocke et al. [104] introduced a systematic design method
that suggests that grind-hardening process was developed in order to overcome and
enhance the limits of today's production technologies.

2.2 Grind-Hardening Process Overview

In industry, a number of different heat treatment methods for the production of the
required surface layer properties are used, as was discussed in Chap. 1. The prob-
lem is that these processes cannot simply be integrated into the production line
thus causing economical disadvantages. Furthermore, the manufacturing of high-
quality steel parts involves usually grinding processes. Grind hardening (Fig. 2.2)
is a process combining the grinding and heat treatment processes into one. It uti-
lizes the friction-generated heat flow, in order to achieve high surface hardness.
The surface hardness of the workpiece is increased by the dissipation of the heat
into the workpiece. The heat dissipation increases the surface temperature of the
workpiece in the austenitic range. Due to high heat flow rates and rapid advance-
ment of the grinding wheel, the workpiece area left behind the grinding wheel is
subjected to rapid quenching, mainly due to heat absorption from inner cold areas
of the workpiece. This self-quenching process induces martensitic transformation
to the workpiece material, resulting in hardness improvement.

   The main process parameters are the workpiece speed, the depth of cut, the cut-
ting speed, the workpiece material and the grinding-wheel type; while the result

Fig. 2.2 Grind-hardening process outline
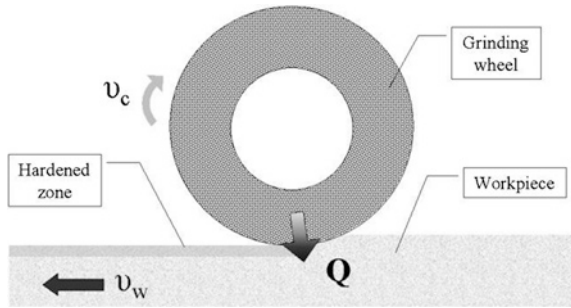
can be described from the hardness penetration depth (HPD) and the surface hardness. Hardness quantitatively represents the degree to which a metal will resist cutting, abrasion, penetration, bending and stretching. HPD on the other hand is the depth beneath the workpiece surface where the hardness has decreased to 80 % of the nominal hardness value on the surface.
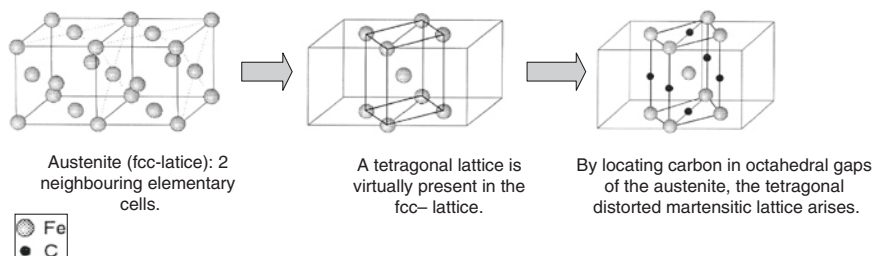
A first concern in grind hardening is the proper selection of process parameters, so as to produce enough heat at the contact zone enabling the heat treatment of the workpiece. Moreover, the proper parameter selection must allow for suitable conditions for the quenching of the material in order to achieve maximum surface hardness.

The surface hardness and the HPD are mainly influenced by the material type and the temperature distribution in the workpiece. The surface hardness depends on the carbon content of the workpiece and the cooling rate. On the other hand, the HPD depends on the temperature field in the workpiece.

2.3 Fundamental Mechanisms in Grind Hardening

Heat treatment methods are utilized in order to alter the technological properties such as the strength, wear resistance, fatigue strength, hardness, impact strength and tendency for brittleness. Steels can be heat treated to produce a great variety of microstructures and thus obtain desired surface properties. The hardening mechanism is based on the phase transformation of austenite to martensite.

The steel before any heat treatment process has ferrite–pearlite structure (face-centred cubic). During grind hardening, heat flow from the contact zone dissipates in the steel, resulting in the increase of the surface temperature. There is a critical temperature at which the carbides in the lamellar pearlite begin to dissolve into iron. As the temperature is raised, more of the carbides are dissolved until the steel consists completely of a solid solution of carbon in iron called austenite (face-centred cubic lattice structure). These critical temperatures where the ferrite–pearlite transformations commences and finishes are depended on the carbon content of the steel and are derived from iron–carbon phase diagrams.

Austenite (fcc-latice): 2 neighbouring elementary cells.

A tetragonal lattice is virtually present in the fcc– lattice.

By locating carbon in octahedral gaps of the austenite, the tetragonal distorted martensitic lattice arises.

Fe
C

Fig. 2.3   Martensite formation

If the austenite-structured steel was left to cool in quasi-state mode, the austenite would be transformed back to ferrite–pearlite structure. Martensite is induced due to the rapid cooling or quenching in order to avoid the diffusion-dependent transformation that produces ferrite–pearlite. The exact cooling conditions that will result in martensite structure in any steel alloy are strongly dependent on carbon content, alloying and austenitic grain size.

The martensitic transformation is characterized by shearing of the austenite lattice (face-centred cube) to the martensite lattice (tetragonal deformed) without diffusion (Fig. 2.3), and therefore, the martensite has exactly the same composition as does its parent austenite, up to 2 % carbon, depending on the alloy composition. Since the diffusion is suppressed, the carbon atoms do not partition themselves between cementite and ferrite-pearlite but instead are trapped in the octahedral sites of the martensitic body-centred cubic structure.

The shear mechanism for the martensite formation is based on the simultaneous and cooperative movement of atoms in contrast to atom-by-atom movement across interfaces during diffusion-dependent transformation.

The critical cooling rate needed for martensite formation, for the case of grind hardening, is reached either by heat dissipation from the austenized surface layer to the cooler workpiece core or by using a coolant fluid. This immediate transformation due to self-quenching presents some advantages in comparison to through-hardening. Grind hardening along with laser hardening and induction hardening are categorized as short-time heat treatment processes due to the very short time required for heating and subsequently quenching. In contradiction to processes that require heating using furnaces and quenching in suitable mediums and are characterized as long-time processes. The heating rate for grind hardening was estimated to be 10^7–10^8 C/s and the heat affecting time is normally less than one second, whereas through heat treatment with all the process cycle times taken into consideration (heating, normalizing, quenching, tempering, etc.) may require up to 24 h processing.

Concerning their homogeneity, short-time austenized, hypoeutectoid steels differ just negligibly from long-time austenized steels, because the subsiding homogenization occurs very quickly (normalization). In short-time treatment of hypereutectoid steels containing higher carbon contents, the risk of overheating the material exists, that could lead to coarser martensite needles and more retained austenite within the hardened structure. In short-time heat treatment processes generally the
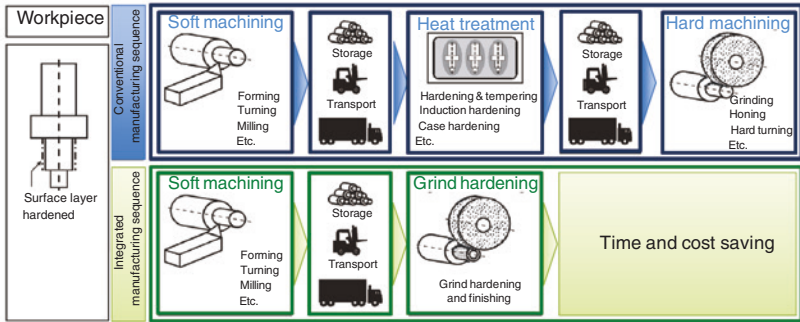
Fig. 2.4 Comparison of a conventional production chain and a production chain including grind hardening

austenizing time is decreased with increasing energy density in the surface layer to avoid melting of the material. As a result, the achievable hardness penetration depth decreases. The thermal aftereffect on martensite is suppressed due to rapid self-quenching, whereby an extremely fine-grained martensitic structure remains.

2.4 Alternative Process Chains

Grind-hardening process makes possible the integration of surface heat treatment not only into the production line, but moreover into the machining process [5]. The result of such integration will be the shortening of the production sequences and the subsequent reduction of the cost. The reduction of cost is justified by the substitution of a number of process steps (less machine set-ups) such as cleaning and transportation to the heat treatment department (Fig. 2.4). Conventional heat treatment methods are not categorized as "eco-friendly" processes due to the excess use of chemical additives, salts and oil quenchants. On the contrary, grind hardening is based on the efficient energy usage philosophy, utilizing the heat generated during grinding to harden the surface layer of the machined part.

2.5 Fundamental Investigations—Feasibility Studies

A number of aspects need to be considered for the controlling of the grind-hardening processes. Some of these aspects can be considered as system parameters and some as grinding process parameters. For example, the systems parameters include the grinding wheel, the grinding fluid, the workpiece material and geometry and the machine tool. On the other hand, the process parameters that need to be considered include the cutting speed, the depth of cut, the feed speed and the grinding fluid supply. Figure 2.5 summarizes the most influencing parameters on grind hardening.
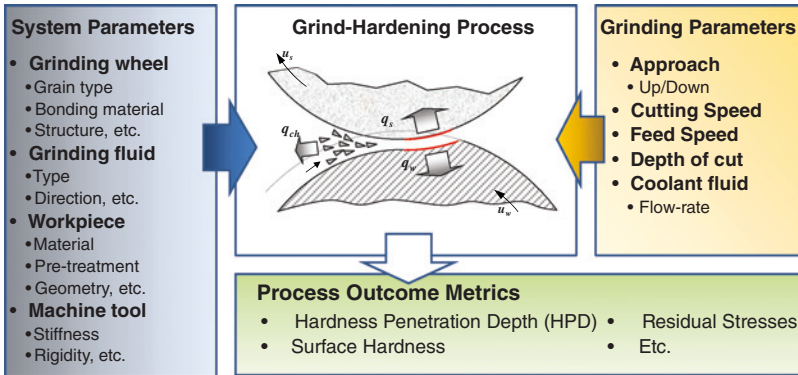
Fig. 2.5 Grind-hardening parameters and the process outcome metrics

2.5.1 Workpiece Material

Fundamental investigations on the process indicate that the hardening result is dependent on the chemical composition and the microstructure of the material, the grinding wheel specification and the process parameters. Conventional heat treatment interrelations are evidenced for grind hardening as well. Generally, martensitic hardenable steels can be ground-hardened. The most applicable metals for grind hardening are the heat-treatable and ball-bearing steels (Table 2.1). The hardening result is determined by the carbon content and the content of alloying elements. The maximum surface hardness that can be obtained is approximately 60 HRC. The comprehensive literature review has shown that research has been conducted on all possible materials (Table 2.2). However, most of the researchers have focused on AISI 52100, AISI 1045, AISI 1065, AISI 4140 and AISI 5140.

AISI 5120 was possibly the first material to be investigated for grind-hardening process [1]. AISI 52100 is a high-carbon, chromium containing low alloy steel and is considered a typical bearing steel alloy. The maximum hardness that can be achieved is usually close to 800 HV with a hardness penetration depth exceeding 300 µm [1, 6]. In a number of studies, though hardness penetration depths close to 1 mm when using lower feed speeds have been reported (indicative sources: [6–8]). In most cases the resulting residual stress profile exhibits compressive stresses close to the surface and can be controlled by careful consideration of the grinding parameters [9].

AISI 1045 is a medium-tensile steel used for a range of different applications such as gears, axles and rolls that require local hardening. It has low through-hardening capability, but can be hardened locally up to hardness levels of 54–60 HRc (400–550 HV). Usually, this hardening takes place through flame or induction hardening. As can be seen in Table 2.2, a number of investigations on grind hardening of this alloy that have been published were reported successful operations. Zurita et al. [10] reported quite lower achievable hardness (up to

Table 2.1 Chemical composition of relevant hardenable steels

Alloy steel designation	Nominal composition (wt%)						
	C	Mn	Si	Cr	Ni	Mo	Fe
AISI 1020	0.17–0.23	0.30–0.60	–	–	–	–	Balance
AISI 1045	0.42–0.50	0.50–0.80	0.17–0.37	≤0.25	≤0.3	–	Balance
AISI 1060	0.55–0.66	0.60–0.90	–	–	–	–	Balance
AISI 1065	0.60–0.70	0.60–0.90	–	–	–	–	Balance
AISI 1066	0.60–0.71	0.80–1.10	–	–	–	–	Balance
AISI 4140	0.38–0.43	0.75–1.00	0.10–0.35	0.80–1.10	≤0.25	0.15–0.25	Balance
AISI 4340	0.37–0.43	0.60–0.80	0.15–0.30	0.70–0.90	1.65–2.00	0.20–0.30	Balance
AISI 5140	0.37–0.44	0.50–0.80	0.17–0.37	0.80–1.10	≤0.030	–	Balance
AISI 52100	0.95–1.05	0.25–0.45	0.15–0.35	1.30–1.65	–	–	Balance
AISI D2	1.5	0.45	0.25	12	–	1	Balance

Table 2.2 Grind hardening studies presented classified per material

Alloy steel designation	Equivalent designation used in the studies	Relevant studies
AISI 1020		[35]
AISI 1045	C45E4, #45	[10–14, 26, 36–48]
AISI 1060		[49]
AISI 1065	65Mn	[15, 16, 50–55]
AISI 1066		[56]
AISI 4140	42CrMo4	[1, 5, 17, 48, 57–60]
AISI 4340		[61]
AISI 5140	40 Cr, 41Cr4, 48MnV	[18–22, 45, 47, 62–72]
AISI 52100	100Cr6	[1, 4–9, 27, 29–33, 48, 73–78]
AISI D2	SKD-11	[23–27]

250 HV); however, Nguyent et al. [11, 12] reported hardness up to 700 HV under dry grind hardening conditions and almost 1,000 HV when assisting the cooling with liquid nitrogen. The typical hardness penetration depth achieved is approximately 0.5 mm (in almost all studies reviewed). The residual stresses profile can be controlled in order to achieve compressive stresses close to the surface of the workpiece [11, 13, 14].

AISI 1065 is a high-carbon steel. Grind hardening of such workpiece materials can result in (close to surface) hardness in the range of 810–870 HV [15, 16]. The achievable hardness penetration can reach up to 2.0 mm as has been reported by Liu et al. [15]. No studies were reported on the residual stresses profile.

AISI 4140 was also among the first workpiece materials to be investigated for grind-hardening process [1, 5]. The maximum achievable hardness is close to 800 HV [1, 5] and the hardness penetration depth that can be achieved is up to 1.0 mm [5]. Fricker et al. [17] presented experimental results of hardness penetration depth values close to 2.0 mm. Compressive residual stresses can be achieved in the white etching areas and the following area of etchable martensite.

Grind hardening of AISI 5140 has been extensively investigated as can be seen in Table 2.2. Hardness can be increased up to 750 HV, with a hardness penetration depth of 1.6 mm [18–20]. Compressive residual stresses can be achieved at the surface of the workpiece material [21, 22].

AISI D2 is a high-carbon, high-chromium tool steel. It can be heat-treated and the hardness can be increased in the range 55-62 HRC. Typically, it is used for manufacturing dies, punches and rolls. Successful grind hardening of such material has been investigated in few studies [23–25]. Finally, one study per AISI 1060, 1066 and 4340 workpiece materials has been presented, and thus no strong conclusions can still be drawn for these alloys.

One of the prerequisites for hardening is sufficient carbon and alloy content. The materials that can be hardened with grind-hardening process usually have at least 0.3 % carbon content. Nevertheless, few papers have been published where successfully grind-hardening alloys of less than 0.3 % carbon content (such as AISI 1020 [26]) is reported.

Furthermore, the initial microstructure (pre-treatment) of the material is critical for the hardening result. In grind hardening, steels in annealed or tempered initial state are hardened. Due to finer dispersion of carbon, tempered initial states lead to reduced diffusion ways and advantageous conditions during austenitization. Deeper hardness penetration depths can be achieved for a tempered material than for an annealed material as pointed out by Brockoff [5] for the case of AISI 52100. Furthermore, the transition from the maximum hardness down to the hardness of the bulk material appears much steeper as for the tempered steel. The tempered material transforms to austenite at lower temperatures, which is equivalent to greater depths beneath the surface in grind hardening. This, furthermore, enables the faster homogenization compared to the austenite formed from the annealed structure.

2.5.2 Workpiece Geometry

Grind-hardening process can be used for selectively heat-treating the surface of both cylindrical and prismatic parts. Most of the papers reviewed focus on the surface grind-hardening process. The key challenge for using this process in complex geometries is the tempering of the already heat-treated surface when the grinding wheel has to pass more than once from the same vicinity. For this reason, the grinding wheel to be used ideally should be wide enough to process all the area. This can be achieved for the case of narrow prismatic parts, as shown by Salonitis et al. [27] for the case of a V-shaped guide.

For the case of cylindrical parts, overlapping is unavoidable as can be seen in Fig. 2.6. This results in tempering of the material, since when the grinding wheel "returns" to the entering point, the already quenched area is reheated in the martensitic range of temperatures. A number of different techniques have been investigated to overcome this problem, such as adaptive control of the grinding wheel rotation speed, modification of the workpiece material (altering the depth of cut) to name few. A recent patent [28] has been granted that attempts to control the overlapping through tangential plunging of the grinding wheel in the workpiece material.
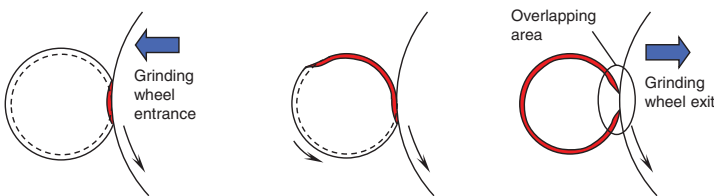

Fig. 2.6 Cylindrical grind-hardening challenge: overlapping area

Table 2.3 Grind hardening studies classified per grinding wheel (listed only the papers where the grinding wheel type is explicitly stated)

Grinding wheel types	References
Corundum	[1, 5–8, 10–15, 19–21, 26, 27, 29–33, 35, 40, 43, 45, 47, 49, 50, 52, 54, 56, 58, 61, 63, 69, 73–75]
CBN	[17, 57, 76, 79, 91]

2.5.3 Grinding Wheel

In grind hardening, the grinding wheel specification influences the heat dissipation and thus the hardening result decisively. In the papers reviewed, 38 reported to have used corundum (aluminium oxide) grinding wheels, and only 4 CBN wheels (Table 2.3). The preference to corundum wheels is due to their lower heat conductivity, allowing thus for more heat to directed in the workpiece material.

Most of the researchers are using fine-grained, resin-bonded corundum wheels of high bond hardness and closed structure. Salonitis et al. documented the effect of the corundum grinding wheel specifications (grain size, hardness and structure) on process forces [29] and hardness penetration depth [30]. Utilization of softer wheels was shown to result in reduced process forces since grain and bonding fracture occurs more easily, and consequently, fewer grains interact with the grinding wheel. Additionally, the hardness penetration depth is increased; this may be attributed to the fact that softer grinding wheels can be more easily deformed and thus, more grains are likely to interact with the workpiece material. The structure number of a grinding wheel represents its porosity; denser grinding wheels were shown to induce higher process forces. The grain size had the smallest effect on the process forces. Grinding wheels with finer grits resulted in higher process forces since more grains are involved in the process, and therefore, more chips are formed, while the cutting forces are increased. However, the hardness penetration depth is reduced since more grains are involved in the process, removing thus more material and thus more heat is removed from the grinding area.

Compared to resin bonded, the use of vitrified bonded wheels can result in heavy loading of the grinding wheel leading to high forces, increased wheel wear and unstable process [5].

CBN and corundum present great differences in terms of the thermal conductivity of the abrasives. Aluminium oxide grains direct the heat towards the workpiece material, whereas the CBN abrasive is able to remove a significant proportion of heat from the grinding zone by heat transfer through the abrasive segments into the steel hub of the wheel [17, 31]. However, CBN can be used for grind hardening, although it has been shown experimentally [17] that there is an upper limit on the workpiece surface speed that can be used.

2.5.4 Process Parameters

Grind hardening process occurs within a small window of process parameters combinations. A number of studies have been published that are focused in defining this process window. Indicatively, Fricker et al. [17] presented a process map (Fig. 2.7) for the case of dry CBN grind hardening of AISI 4140. Salonitis [7, 32] presented process maps for the case of both dry and wet grind hardening of AISI 52100 with corundum wheel (Fig. 2.8). The available maps can be used for selecting the process parameters based on the design requirements (such as hardness penetration depth) and the limitations set by the grinding machine. Salonitis et al. [27] used these process maps for selecting the process parameters for the grind hardening of a V-shaped guide. The process for deriving these process maps is described in detail in the Chap. 3 of the present book.

An interesting theoretical process limitation is the maximum achievable hardness penetration depth. Salonitis and Chryssolouris [33] estimated the maximum

Fig. 2.7 Process map for the occurrence of grind hardening of AISI 4140 using a CBN grinding wheel (based on the results presented in [17])
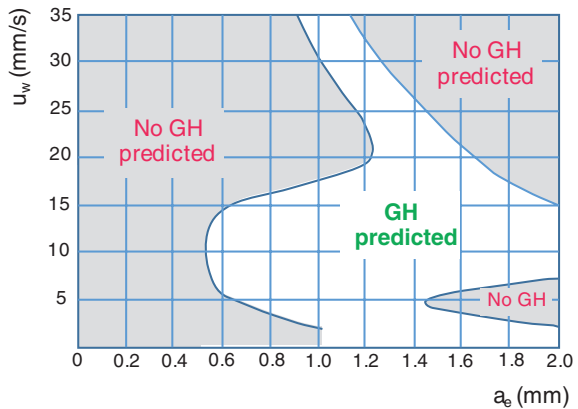
Fig. 2.8 Process map for selecting parameters combination for the grind-hardening of AISI 5120 using corundum grinding wheels [30]
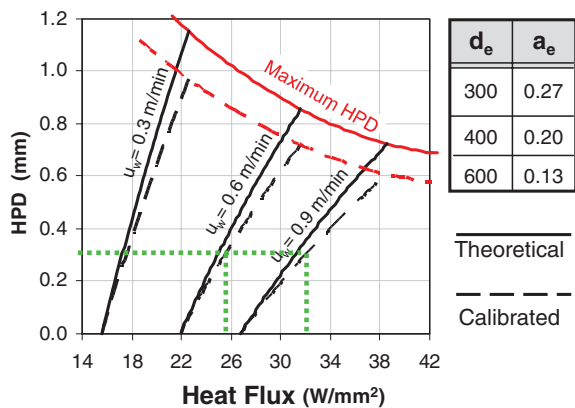
depth based on the assumption that this will occur when the surface temperature reaches the melting temperature. This limit is depicted in the process maps developed as can be seen in Fig. 2.8.

It is thus obvious that the hardening result can be controlled by the process parameters with most important ones being the depth of cut and the feed speed. Furthermore, the cutting speed (grinding wheel speed) can be used for controlling the process.

- **Depth of cut**
  In surface grinding with constant feed speed, the depth of cut is proportional to the specific material removal rate as well to the equivalent chip thickness. For constant specific material removal rate, an increase of the depth of cut results in deeper HPD (Fig. 2.9). The maximum HPD is achieved in the transition area between the pendulum and creep feed grinding. A further increase of the depth of cut leads to decreasing HPD in the area of creep feed grinding.

To maximize the HPD in grind hardening, high depths of cut have to be applied. On the other hand, such a procedure will be limited by the spindle power of the machine tool and the required accuracy of the workpiece. Furthermore, too high energy inputs to the workpiece could lead to undesired alterations in the material like hardening cracks or tempered zones at the surface. For industrial applications, the depth of the cut needs to be optimized for each component considering its special demands and operational loadings.

- **Feed speed**
  The feed speed is directly affecting the heat entering the part. For very low feed speeds, the generated grinding power and thus the generated heat is too low for the austenitization. When increasing feed speed, the generated heat and the HPD increases (Fig. 2.9). A further increase of the feed speed results in shorter contact times leading to decreasing HPDs. Thus, maximum HPD can be achieved in for medium feed speeds.
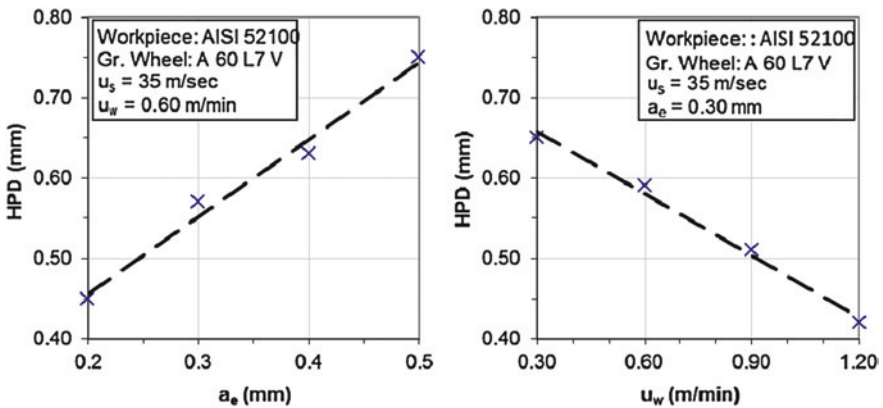

Fig. 2.9 Depth of cut and workpiece speed effect on hardness penetration depth (based on the experimental data presented in [33] for AISI 52100)

- **Cutting speed**
  The influence of the cutting speed is quite complex. The increased cutting speeds lead to partly decreasing cutting powers, while in some ranges the opposite occurs.

In a number of studies the effect of the process parameters on the surface quality of the processed workpiece has been presented as well. Indicatively, the impact on burr formation has been discussed [94, 106, 107]. Chamfer is also of interest with regards the impact it has to the achievable hardness distribution [107, 108].

2.6 Simulation of the Grind-Hardening Process

Modeling and simulation of grinding processes has been thoroughly reviewed [34]. Grind-hardening process modelling, being an abrasive process, was based on the models presented for relevant grinding processes. 50 papers out of the 112 reviewed presented models for predicting one or more aspects of the grind-hardening process. Most of the models presented for the estimation of temperature distribution within the workpiece material and the subsequent estimation of hardness penetration depth and/or residual stresses are based on finite element method. However, estimation of the heat generated between the grinding wheel and the workpiece material is in most cases either calculated empirically or using analytical models.

In the following Table 2.4, the classification of the papers based on the type of analysis (FEA or analytical), modelling dimensions, modelled attribute response

Table 2.4 Grind hardening simulation-modelling studies

Modelling method	Modelled attribute					
	Process forces	Temperature	Phase transformation	Surface hardness	HPD	Residual stresses
FEA—2D	–	[4, 6, 7, 9, 12–14, 21, 22, 27, 30–33, 35, 38, 39, 64–66, 69, 74, 76, 78, 80–87, 111]	[4, 9, 12, 65, 76, 82, 110]	[35, 57, 74, 76, 82, 85]	[6, 7, 27, 30–33, 35, 66, 74, 99, 100]	[4, 9, 13, 14, 21, 22, 76, 82, 85]
FEA—3D	–	[8, 27, 32, 37, 40, 41, 43, 47, 67, 68, 75, 78, 88, 89]	[8, 32, 40, 43, 75, 78]	[32, 40, 43, 78]	[27, 32, 40, 67, 68]	[89]
Analytical	[8, 29, 30, 32, 42, 69, 73]	[17, 36, 96–98]	[17, 20, 32, 78]	–	–	–
Empirical	[6, 31]	[102]	[7, 32, 33, 105, 112]	[7, 32, 33, 109]	[90, 95]	–

(temperature, forces, HPD, residual stresses, etc.). In the following chapter that focusses on the grind-hardening process modelling, these models are reviewed in more detail.

Further to the modelling and simulation of the process mechanics, a number of studies have been focused also on the environmental impact of the grind-hardening and the benefits gained by combining heat treatments with grinding. Chapter 4 will present in detail the state of the art, however for the sake of completeness, a brief overview will be given here as well. The benefits with regards the resource efficiency have been highlighted by Reinhart et al. [103]. Salonitis et al. in a number of studies focused on the environmental impact assessment using both life cycle assessment [93] and energy audits [77, 101]. Few other studies on the ecological merits of grind-hardening have been presented as well [92].

2.7 Challenges for Future

Although, grind hardening is a highly innovative process, industrial introduction is restricted by a number of factors. One of the main open issues of today's state of the art of grind-hardening technology is the formation of overlapping areas. Overlapping areas which can also occur in induction hardening are generated in cylindrical grinding after one revolution of the workpiece when an area which was already grind hardened is again thermally influenced by the grinding process. Particularly, in cylindrical grind hardening, improper junction of the hardened surface layer is generated in overlapping areas. In the overlapping area, the hardened surface layer material is annealed, resulting in reduced hardness and decreased hardness penetration depth. Thus grind-hardening technology today is limited to applications where overlapping areas are not generated like surface grinding applications or where the occurrence of overlapping areas can be accepted; for example, in the area of bearing fits or runways for packing rings. An important task of the proposed research project is the further development of such strategies and application in grinding tests.

A general limiting factor of grind hardening is the HPD, which is technologically restricted to about 2.5 mm due to high grinding forces and physical properties of the material. Furthermore, grind-hardening technology is restricted by the wear of the grinding wheel resulting in relative low G-ratios (grinding ratio) and decreased cost savings.

During the last years, the research on grind hardening has been focused on various aspects of the process such as the use of liquid nitrogen for the quenching of the part. The modelling of the process using hybrid analytical and finite element analysis methods was first introduced by Salonitis in a number of studies [7, 13, 14, 27, 30, 32, 33] and similar attempts have been presented recently by Zhang et al. and Kolkwitz et al. However, a number of issues have not yet been modelled such as residual stresses formation and geometry deformation.

References

1. Brinksmeier E, Brockhoff T (1996) Utilization of grinding heat as a new heat treatment process. CIRP Ann Manuf Technol 45:283–286
2. Eda H, Ohmura E, Yamauchi S (1993) Computer visual simulation on structural changes of steel in grinding process and experimental verification. CIRP Ann Manuf Technol 42(1):389–392
3. Shaw MC, Vyas A (1994) Heat-affected zones in grinding steel. CIRP Ann Manuf Technol 43(1):279–282
4. Zhang L, Mahdi M (1995) Applied mechanics in grinding—IV. The mechanism of grinding induced phase transformation. Int J Mach Tools Manuf 35(10):1397–1409
5. Brockhoff T (1999) Grind-hardening: a comprehensive view. CIRP Ann Manuf Technol 48(1):255–260
6. Chryssolouris G, Tsirbas K, Salonitis K (2005) An analytical, numerical, and experimental approach to grind hardening. J Manuf Process 7(1):1–9
7. Salonitis K, Chryssolouris G (2007) Cooling in grind-hardening operations. Int J Adv Manuf Technol 33(3-4):285–297
8. Foeckerer T, Kolkowitz B, Heinzel C, Zaeh MF (2012) Experimental and numerical analysis of transient behavior during grind-hardening of AISI 52100. Prod Eng Res Devel 6(6):559–568
9. Shah SM, Nelias D, Zain-ul-abdein M, Coret M (2012) Numerical simulation of grinding induced phase transformation and residual stresses in AISI-52100 steel. Finite Elem Anal Des 61:1–11
10. Zurita O, Acosta A, Moreno D (2003) Superficial hardening in the plane grinding of AISI 1045 steel. J Mater Eng Perform 12(3):298–303
11. Nguyen T, Zarudi I, Zhang LC (2007) Grinding-hardening with liquid nitrogen. Int J Mach Tools Manuf 47:97–106
12. Nguyen T, Zhang LC (2010) Grinding–hardening using dry air and liquid nitrogen. Int J Mach Tools Manuf 50:901–910
13. Salonitis K (2014) On surface grind hardening induced residual stresses. Procedia CIRP 13:264–269
14. Salonitis K, Kolios A (2015) Experimental and numerical study of grind hardening induced residual stresses on AISI 1045 Steel. Int J Adv Manuf Technol. doi:10.1007/s00170-015-6912-x
15. Liu JD, Wang GC, Wang Z, Fan ST (2006) Experimental research on grind-hardening of 65Mn steel. Mater Sci Forum 505–507:787–792
16. Liu LF, Zhuang JZ, Huang SW, Xu ZL (2010) Influence of original structure on the grind-hardened layer structure and its property of 65Mn steel. Key Eng Mater 455:580–584
17. Fricker DC, Pearce TRA, Harison JL (2004) Predicting the occurrence of grind hardening in cubic boron nitride grinding of crankshaft steel. Proc Inst Mech Eng Part B: J Eng Manuf 218:1339–1355
18. Xiao B, Park YC, Su HH, Ding WF, Fu YC, Xu JH (2006) The influence of grinding parameters on the superficial hardening effect of 48MnV microalloyed steel. Key Eng Mater 315–316:15–19
19. Han Z, Zhang N, Gao D, Yang G (2007) Research into grinding hardening of microalloyed non-quenched and tempered steel. J China Univ Mining Technol 17(2):238–241
20. Xiao B, Su HH, Li SS, Xu HJ (2007) Research on grind-hardening temperature and cooling rate of 48MnV microalloyed steel. Key Eng Mater 359–360:148–152
21. Zhang L, Ge P, Bi W, Zhang Q (2011) Experiment and simulation on residual stress of surface hardened layer in grind-hardening. Solid State Phenom 175:166–170
22. Li SS, Xiao B, Su HH, Gong SL (2012) Simulation on grind-hardening residual stress field of 48MnV steel. Key Eng Mater 499:301–306

23. Ming WW, Liu G, Chen M (2007) Experimental study on the hardened surface layer of grinding SKD-11 hardened steel. Key Eng Mater 359–360:224–228
24. Ming WW, Liu G, Chen M (2007) Study on surface grind-hardening of SKD-11 hardened steel. Int J Manuf Tech Manag 12(1/2/3):236
25. Ming WW, An QL, Chen M (2008) Study on the effect of grinding parameters to the white layer formation in grinding SKD-11 hardened steel. Adv Mater Res 53–54:279–284
26. Yang G, Han Z, Du C (2009) External grind-hardening experiments and its grinding force. J Shanghai Univ (English Ed) 13(2):169–173
27. Salonitis K, Stavropoulos P, Stournaras A, Chryssolouris G (2007) Finite element modeling of grind hardening process. In: Proceedings of the 10th CIRP international workshop on modeling of machining operations, Calabria, Italy, pp 117–123
28. Niemeyer B, Foeckerer T, Chaphalkar N, Hyatt GA (2013) Grind hardening method and apparatus. US Patent with Pub. No.: US 2013/0273811 A1
29. Salonitis K, Stavropoulos P, Kolios A (2014) External grind-hardening forces modelling and experimentation. Int J Adv Manuf Technol 70(1–4):523–530
30. Salonitis K, Chondros T, Chryssolouris G (2008) Grinding wheel effect in the grind-hardening process. Int J Adv Manuf Technol 38:48–53
31. Tsirbas K (2002) Theoretical and experimental investigation of grind-hardening process. Ph.D. dissertation, Patras University (in Greek http://nemertes.lis.upatras.gr/jspui/bitstream /10889/301/1/76.pdf)
32. Salonitis K (2006) A methodology for the prediction of the hardness distribution and the hardness penetration depth caused by grind-hardening process. Ph.D. dissertation, Patras University (in Greek http://nemertes.lis.upatras.gr/jspui/bitstream/10889/1430/1/Nimertis_S alonitis%28a%29.pdf)
33. Salonitis K, Chryssolouris G (2007) Thermal analysis of grind-hardening process. Int J Manuf Technol Manage 12(1/2/3):72–92
34. Toenshoff HK, Peters J, Inasaki I, Paul T (1992) Modelling and simulation of grinding processes. CIRP Ann Manuf Technol 41(2):677–688
35. Zhang J, Ge P, Jen T-G, Zhang L (2009) Experimental and numerical studies of AISI1020 steel in grind-hardening. Int J Heat Mass Transf 52:787–795
36. Efremov VD, Zheludkevich MS, German ML (2000) Computer thermal model for hardening grinding. J Eng Phys Thermophys 73(2):428–435
37. Nguyen T, Zhang LC (2009) Temperature fields in workpieces during grinding-hardening with dry air and liquid nitrogen as the cooling media. Adv Mater Res 76–78:3–8
38. Nguyen T, Zhang LC, Le SD (2011) Heat transfer in grinding-hardening of a cylindrical component. Adv Mater Res 325:35–41
39. Nguyen T, Zhang LC (2011) Prediction of the hardened layer in traverse cylindrical grinding-hardening. Mater Sci Forum 697–698:13–18
40. Nguyen T, Zhang LC (2011) Realisation of grinding-hardening in workpieces of curved surfaces: Part 1: Plunge cylindrical grinding. Int J Mach Tools Manuf 51:309–319
41. Li J, Liu S, Du C (2013) Experimental research and computer simulation of face grind-hardening technology. Strojniški vestnik - J Mech Eng 59(2):81–88
42. Han ZT, Yang G, Luo HB (2013) Grinding-hardening experiments and grinding force analysis in infeed external grinding for 45 steel. Adv Mater Res 753–755:281–286
43. Hyatt GA, Mori M, Foeckerer T, Zaeh MF, Niemeyer N, Duscha M (2013) Integration of heat treatment into the process chain of a mill turn center by enabling external cylindrical grind-hardening. Prod Eng Res Devel 7(6):571–584
44. Yuan W, Liu JD, Xu ZL (2013) Orthogonal experimental study on the grinding-hardened layer's depth and its uniformity of 45 steel. Adv Mater Res 668:898–901
45. Yang G, Han ZT, Du CL (2014) Comparative study on the external grind-hardening experiments of 40Cr steel and 45 steel. Adv Mater Res 971–973:26–29
46. Alonso U, Ortega N, Sanchez JA, Pombo I, Plaza S, Izquierdo B (2014) In-process prediction of the hardened layer in cylindrical traverse grind-hardening. Int J Adv Manuf Technol 71(1–4):101–108

47. Songyong L, Gang Y, Jiaqiang Z, Xiaohui L (2014) Numerical and experimental studies on grind-hardening cylindrical surface. Int J Adv Manuf Technol (published online)
48. Alonso U, Ortega N, Sanchez JA, Pombo I, Izquierdo B, Plaza S (2015) Hardness control of grind-hardening and finishing grinding by means of area-based specific energy. Int J Mach Tools Manuf 88:24–33
49. Liu J, Yuan W, Huang S, Xu Z (2012) Experimental study on grinding-hardening of 1060 steel. Energy Procedia 16:103–108
50. Liu LF, Zhuang JZ, Liu C (2011) Influence of depth of cut on grind-hardened layer and its uniformity. Appl Mech Mater 109:345–349
51. Liu JD, Zhuang JZ, Huang SW (2011) Influence of the grinding pass on microstructure and its uniformity of the grind-hardened layer. Adv Mater Res 211–212:36–39
52. Zhuang JZ, Liu LF, Zhang YZ (2011) Study on depth and its uniformity of 65Mn steel grind-hardened layer. Key Eng Mater 487:94–98
53. Liu J, Zhuang J, Xiong J (2011) Study on grinding force of grind-hardening based on orthogonal experimental method. In: The proceedings of the second international conference on mechanic automation and control engineering (MACE), pp 1676–1678
54. Liu J, Xiong J, Yuan W (2012) Experiment study on grinding force of 65Mn steel in grinding-hardening machining. In: Future control and automation, pp 239–246
55. Liu JD, Yuan W, Xiong JK, Huang SW (2012) Quality and control of grinding-hardening in workpieces. Key Eng Mater 522:87–91
56. Liu JD, Wang GC, Wang BL, Chen KM (2007) Study on the formation of grind-hardening of steel AISI 1066. Eng Mater 329:57–62
57. Hou YL, Li CH, Ding YC (2009) An investigation into integrate the surface hardening with the grinding precision finishing. Key Eng Mater 407–408:560–564
58. Ma Z, Liu KM, Zhang LY (2011) Study on the structure of grind-hardened layer and parameter of hardening depth of 42CrMo steel. Adv Mater Res 189–193:969–973
59. Liu KM, Zhang LY, Ma Z, Liu B (2012) Research on the properties of grind-hardening and abrasion of 42CrMo steel in agricultural diesel engine crankshaft. Adv Mater Res 619:567–571
60. Zhang LY, Sun FH, Jiang YH (2012) Research on the structure and wear properties of grind-hardened 42CrMo. Adv Mater Res 619:561–566
61. De Lima A, Gambaro LS, Vieira M, Baptista EA (2011) The use of cylindrical grinding to produce a martensitic structure on the surface of 4340 steel. J Braz Soc Mech Sci Eng 33(1):34–40
62. Liu JD, Wang GC, Li QF, Pei HJ, Jia ZH, Wang Z (2006) Research of surface hardening based on transverse feed grinding. Mater Sci Forum 532–533:584–587
63. Wang GC, Liu JD, Pei HJ, Jia ZH, Ma LJ (2006) Study on forming mechanism of surface hardening in two-pass grinding 40Cr steel. Key Eng Mater 304–305:588–592
64. Zhang L, Ge PQ, Zhang JH, Zhu ZJ, Luan ZY (2007) Experimental and simulation studies on temperature field of 40Cr steel surface layer in grind-hardening. Int J Abras Technol 1(2):187–197
65. Wang GC, Pei HJ, Zhang JY, Zhang CY, Li QF (2008) Formation and control of 40Cr grind-hardening. Key Eng Mater 373–374:758–761
66. Li SS, Xiao B, Qin SX, Song ZH, Su HH, Gong H (2008) Investigation on simulation for grind-hardening temperature field of non-quenched and tempered steel. Key Eng Mater 375–376:520–524
67. Zhang R, Ge P, Zhang L, Li B, Zhao C (2010) Numerical simulation of temperature field for rack grind-hardening. Adv Mater Res 135:200–204
68. Zhang L, Gao Y, Bi W (2010) Simulation and prediction studies on harden penetration depth of AISI 5140 alloy steel in surface grinding. Appl Mech Mater 29–32:1898–1901
69. Zhang Z, Ge P, Zhang L, Tian M (2010) Study on grind-hardening temperature field based on infrared temperature measurement and numerical simulation. Key Eng Mater 443:394–399

70. Liu J, Yuan W (2012) Experimental study on wear test of grind-hardened layer. Adv Mater Res 562–564:115–118
71. Han ZT, Yang G, Luo HB (2014) Research on grind-hardening process through integration of physical experiments and dynamic simulation. Adv Mater Res 941–944:1570–1573
72. Yang G, Han ZT, Du CL (2014) Study on external grind-hardening experiments and the analysis of hardening effects for 40Cr steel. Appl Mech Mater 597:223–227
73. Chryssolouris G, Salonitis K (2004) Theoretical Investigation of the grinding wheel effect on grind hardening process. In: Proceedings of the IFAC-MIM'04 conference on manufacturing, modelling, management and control, Athens, Greece
74. Zah MF, Brinksmeier E, Hainzel C, Huntemann J-W, Fockerer T (2009) Experimental and numerical identification of process parameters of grind-hardening and resulting part distortions. Prod Eng Res Devel 3(3):271–279
75. Kolkwitz B, Foeckerer T, Heinzel C, Zaeh MF, Brinksmeier E (2011) Experimental and numerical analysis of the surface integrity resulting from outer-diameter grind-hardening. Procedia Engineering 19:222–227
76. Duscha M, Eser A, Klocke F, Broeckmann C, Wegner H, Bezold A (2011) Modeling and simulation of phase transformation during grinding. Adv Mater Res 223:743–753
77. Salonitis K (2012) Efficient grinding processes: an energy efficiency point of view. In: Proceedings of the 10th international conference on manufacturing research (ICMR 09), Birmingham, pp 541–546
78. Foeckerer T, Zaeh MF, Zhang OB (2013) A three-dimensional analytical model to predict the thermo-metallurgical effects within the surface layer during grinding and grind-hardening. Int J Heat Mass Transf 56(1–2):223–237
79. Luo SY, Wu SQ, Hsu FJ (2011) Analysis of the vitrified CBN wheels for the performance of grinding hardened steel. Adv Mater Res 264–265:937–942
80. Zhang L, Ge PQ, Zhang JH, Zhang Q (2007) Study on hardness depth variation of different grinding zone in grind-hardening. Adv Mater Res 24–25:333–336
81. Wang GC, Pan ZF, Jin Y, Zhang CL, Hua J, Liu D (2009) Finite element prediction of grind-hardening layer thickness. Key Eng Mater 416:253–258
82. Ge PQ, Zhang Q, Zhang L, Zhang JH (2009) Prediction of the residual stress in grind-hardening with thermal-mechanical-phase transformation stress coupled analysis. Mater Sci Forum 626–627:345–350
83. Nguyen T, Zhang LC (2010) Understanding the temperature field in plunge cylindrical grinding for grinding-hardening. Key Eng Mater 443:388–393
84. Zhang Y, Ge PQ, Zhang L (2011) Numerical analysis of surface temperature in grind-hardening based on time variation heat flux. Mater Sci Forum 697–698:34–38
85. Zhang Y, Ge PQ, Zhang L, Jiang JL (2012) The numerical simulation for thermal deformation in grinding hardening thin workpiece. Key Eng Mater 501:500–504
86. Cheng W, Liang P (2013) Design of automatic control system of grinding zone temperature in grinding hardening. Key Eng Mater 589–590:723–728
87. Liu JD, Yuan W, Xu ZL, Yu DM (2013) Numerical simulation of grinding-hardened layer's depth in the reciprocating grinding of 45 steel. Appl Mech Mater 401–403:656–659
88. Wang GC, Hua CL, Zou JF, Pei HJ, Huang J (2014) Characteristic of residual stress distributions at workpiece surface in grind-hardening. Appl Mech Mater 494–495:624–627
89. Zhang Y, Ge P, Be W (2015) Plane grind-hardening distortion analysis and the effect to grind-hardening layer. Int J Adv Manuf Technol (published online)
90. Tsirbas K, Mourtzis D, Chryssolouris G (1999) Grind-hardening modeling with the use of neural networks. In: Proceedings of the 5th international conference on advanced manufacturing systems and technology, Udine, Italy, pp 289–300
91. Stöhr R, Heinzel C (2002) Grind-hardening with CBN. Grind Abras Mag 06–07(2002):22–30
92. Liu ZQ, Xing A, Wang ZH (2006) A comparison study of surface hardening by grinding versus machining. Key Eng Mater 304–305:156–160

93. Salonitis K, Tsoukantas G, Drakopoulos S, Stavropoulos P, Chryssolouris G (2006) Environmental impact assessment of grind-hardening process. In: Proceedings of the 13th CIRP international conference on life cycle engineering, Leuven, Belgium, pp 657–662

94. Wang GC, Liu JD, Li QF, Zhu YM, Pei HJ, Zhang JY (2007) Formation and control of burr in grind-hardening. Key Eng Mater 359–360:98–102

95. Pan ZF, Wang GC, Hua CL, Pei HJ (2009) Research and development of LM neural network prediction system for grind-hardening. Eng Mater 416:248–252

96. Zhang ZG, Ge PQ, Zhang L, Bi WB (2010) A study on critical heat flux in grind-hardening. Key Eng Mater 431–432:130–133

97. Zhang L, Bi WB, Zhang RB (2010) An approximate solution of energy partition in grind-hardening process. Adv Mater Res 135:298–302

98. Zhang JH, Zhang XJ, Yu GY, Gu ML, Ge PQ (2010) An investigation on the heat partitioning in grind-hardening. Adv Mater Res 97–101:2095–2098

99. Zhang L, Xu XH, Yan CF (2010) Analysis of grinding parameters on hardness layer depth. Appl Mech Mater 37–38:131–134

100. Liu JD, Zhuang JZ, Zhang XL, Xu ZL (2010) Influence of grinding parameters on the depth and uniformity of cylindrical grinding-hardened layer. Adv Mater Res 102–104:733–737

101. Salonitis K (2015) Energy efficiency assessment of grinding strategy. Int J Ene Sec Manag 9(1):20–37

102. Cheng W, Wang Gui Cheng, Liang P (2011) Automatic control technology of grinding zone temperature in grinding hardening. Adv Mater Res 381:48–51

103. Reinhart G, Reinhardt S, Föckerer T, Zäh MF (2011) Comparison of the Resource Efficiency of alternative process chains for surface hardening. In: Globalized solutions for sustainability in manufacturing, pp 311–316

104. Klocke F, Roderburg A, Zeppenfeld C (2011) Design methodology for hybrid production processes. Procedia Engineering 9:417–430

105. Xiu SC, Liu MH, Wei JH (2012) Analysis of microstructure of grinding strengthening layer in point grinding under small depth of cut conditions. Adv Mater Res 472–475:974–977

106. Liu JD, Yuan W, Xiong JK, Xu ZL, Huang SW (2012) Study on the two-side direction burr in grinding-hardening machine based on orthogonal experimental method. Appl Mech Mater 217–219:1869–1873

107. Liu JD, Yuan W, Xiong JK, Xu ZL (2013) Influence of chamfer size on the two-side direction burr formed in grinding-hardening machine. Adv Mater Res 645:392–395

108. Liu JD, Yuan W, Xiong JK, Xu ZL (2013) Influence of grinding parameters and chamfer size on the grinding-hardened layer's depth. Adv Mater Res 718–720:1569–1572

109. Liu JD, Yuan W, Chen M (2013) Influence of workpiece's size on the structure and performance of grinding-hardened layer. Key Eng Mater 579–580:56–60

110. Liu M, Nguyen T, Zhang LC, Qiong W, Le Sun D (2014) On the profile and microstructure variations of grinding-induced hardening layer in a cylindrical workpiece. Adv Mater Res 1017:3–8

111. Li H, Zou JF, Wang GC (2014) Prediction of thermal gradient in traverse cylindrical grind-hardening. Appl Mech Mater 590:280–283

112. Liu JD, Zhuang JZ, Xu ZL (2014) Study on the grind-hardening of the loader clevis pin. Key Eng Mater 621:140–145